Cosmic Abundances as Records of Stellar Evolution and Nucleosynthesis
ASP Conference Series, Vol. XXX, 2005
F.N. Bash and T.G. Barnes (editors)

The solar chemical composition

Martin Asplund[1]

[1]*Research School of Astronomy and Astrophysics, Australian National University, Cotter Road, Weston 2611, Australia*

Nicolas Grevesse[2]

[2]*Centre Spatial de Liège, Université de Liège, avenue Pré Aily, B-4031 Angleur-Liège, Belgium and Institut d'Astrophysique et de Géophysique, Université de Liège, Allée du 6 Août, 17, B5C, B-4000 Liège, Belgium*

A. Jacques Sauval[3]

[3]*Observatoire Royal de Belgique, avenue circulaire, 3, B-1180 Bruxelles, Belgium*

Abstract. We review our current knowledge of the solar chemical composition as determined from photospheric absorption lines. In particular we describe the recent significant revisions of the solar abundances as a result of the application of a time-dependent, 3D hydrodynamical model of the solar atmosphere instead of 1D hydrostatic models. This has decreased the metal content in the solar convection zone by almost a factor of two compared with the widely used compilation by Anders & Grevesse (1989). While resolving a number of long-standings problems, the new 3D-based element abundances also pose serious challenges, most notably for helioseismology.

1. Introduction

The chemical composition of the Sun is one of the most important yardsticks in astronomy with implications for basically all fields from planetary science to the high-redshift Universe. Standard practise is to compare the element content in a cosmic object with the corresponding value for the Sun using the normal logarithmic abundance scale $[\mathrm{X/H}] \equiv \log\left(N_\mathrm{X}/N_\mathrm{H}\right)_* - \log\left(N_\mathrm{X}/N_\mathrm{H}\right)_\odot \equiv \log\epsilon_{\mathrm{X},*} - \log\epsilon_{\mathrm{X},\odot}$. Abundance ratios such as [C/Fe] are defined correspondingly. Hydrogen is the chosen reference element since it is the most common element in the Universe as a whole and that it normally dominates the continuous opacity in the formation of the stellar spectra. The solar abundances are, however, not only of interest as a reference point in astronomy but are also of profound importance for the understanding of our own solar system and the solar interior.

Most of our knowledge of the overall abundance distribution of the elements in the solar system originates in two quite different sources: the solar photospheric spectrum and pristine meteorites, in particular the so-called C1

chondrites[1] (e.g. Anders & Grevesse 1989). Each has their own advantages and disadvantages. The abundances of a very large number of elements can be determined using absorption lines in the solar spectrum. However, since the results are dependent on having realistic models of the solar atmosphere and the line formation process the accuracy can only be expected to be good at the 10% (0.04 dex) level at best. Isotopic abundance information is only available in very rare instances. Model-independent meteoritic isotopic abundances can be measured to exquisite accuracy in the laboratory but only a very small subsample of meteorites do not show effects of fractionation. In addition, elements like H, He, C, N, O and Ne are all volatile and hence depleted in the meteorites. It is therefore clear that the two methods complement each other well. The present review will describe our knowledge of the solar photospheric chemical composition, in particular in light of recent significant revisions of these abundances following the application of the new generation of three-dimensional (3D) hydrodynamical model atmospheres to the problem.

2. Model Atmospheres, Line Formation and Other Obstacles

While the chemical composition of a star is encoded in its spectrum, it is not immediately extractable without first modelling the stellar atmosphere and the line formation process. Since stellar element abundances are thus not observed but derived they are by necessity model-dependent. As more realistic modelling become available the estimated stellar abundances may therefore change with time. Equally important is improved atomic and molecular data, which is nicely exemplified by Sneden et al. in these proceedings. Obviously progress in both of these areas is vital. Indeed they are also complementary as more realistic modelling can uncover shortcomings in the input physics and vice versa.

Traditionally, standard stellar abundance analyses employ time-independent, one-dimensional (1D) model atmospheres in hydrostatic equilibrium. Such models basically come in two types: theoretical and semi-empirical. In the former the temperature structure is computed assuming flux constancy, i.e. the same energy is transported through each atmospheric layer. The energy is assumed to be carried solely by radiation or convection. For simplicity, the convective energy flux is approximated with the local mixing length theory (Böhm-Vitense 1958) or some close relative thereof (e.g. Canuto & Mazzitelli 1991). In the absence of convection, radiative equilibrium holds. It is crucial to include the effects of blanketing from spectral lines when integrating the radiative transfer equation over all wavelengths in order to obtain a realistic temperature structure. LTE is normally assumed for the computation of the atomic populations and the radiative transfer. Some of the most widely-used theoretical 1D model atmospheres for late-type stars are those by Kurucz (1979), the MARCS consortium (Gustafsson et al. 1975) and the Phoenix team (Hauschildt et al. 1999), which are all continuously improving their models, mainly through the inclusion of better and more complete atomic and molecular physics.

[1]Important and complementary information is provided by studies of for example the solar corona, solar wind, solar energetic particles, solar flares and lunar soil, which however will not be discussed here.

In a semi-empirical model atmosphere the temperature is deduced from observations through an inversion procedure, normally using spectral lines of different line formation depths and/or center-to-limb variations. It therefore follows that the atmosphere in such a model does not need to obey flux constancy nor is it necessary to estimate the radiative and convective energy transport. The danger with such a method is that the line formation calculations may be faulty, for example due to the assumption of LTE or the use of erroneous line data. This would directly translate to an incorrect temperature structure. Hydrostatic equilibrium is assumed also in semi-empirical model atmospheres. Likewise, a knowledge of the equation-of-state is necessary to relate temperature, gas pressure and electron pressure. Semi-empirical atmosphere modelling has only been tried relatively few times for stars other than the Sun (e.g. Allende Prieto et al. 2000) but is a relatively common practise in solar analyses. Two of the most widely used solar semi-empirical models are the VAL-3C (Vernazza et al. 1976), and Holweger-Müller (1974) models. The former is optimised for chromospheric studies while the latter has traditionally been the model of choice for solar abundance analyses.

More recently, a new generation of time-dependent 2D and 3D hydrodynamical model atmospheres has become available and applied in stellar abundance analyses (e.g. Nordlund & Dravins 1990; Dravins & Nordlund 1990; Steffen et al. 1995; Atroshchenko & Gadun 1994; Stein & Nordlund 1998; Asplund et al. 1999, 2000a,b, 2004a,b; Asplund 2000, 2004; Asplund & García Pérez 2001; Steffen & Holweger 2002; Vögler et al. 2004). By simultaneously solving the standard hydrodynamical equations for conservation of mass, momentum and energy together with the 3D radiative transfer equation, both the radiative and convective energy transport are self-consistently computed. No mixing length theory with its free parameters therefore enters the modelling. The effects of line-blanketing are accounted for through the use of opacity binning assuming LTE (Nordlund 1982). State-of-the-art equation-of-state (e.g. Mihalas et al. 1988) and opacities (e.g. Kurucz 1993; Cunto et al. 1993) are used. One can easily imagine that for late-type stars such as the Sun where the convection zone reaches up to and even beyond the optical surface, such 3D hydrodynamical modelling is necessary to capture the time-dependence and resulting atmospheric inhomogeneities of granulation. Being more sophisticated does not, however, necessarily make such 3D models more realistic. A great deal of effort lately has therefore been invested in testing the predictions of these models against an arsenal of observational constraints, in particular for the Sun. So far the comparison has been very satisfactory, which gives confidence in the realism of the 3D models and their predictions (e.g. Stein & Nordlund 1998). For example, the intrinsic Doppler shifts inherent in the hydrodynamical modelling render the classical concepts of micro- and macroturbulence obsolete, yet the theoretical 3D line profiles agree essentially perfectly with the observed profiles, including their line shifts and asymmetries (e.g. Asplund et al. 2000a).

Besides the atmospheric modelling, it is also necessary to accurately model the line formation and the radiative and collisional processes that couple the radiation field with the gas. Most analyses are based on the assumption of LTE, which simplifies matter immensely by assuming that the atomic populations are described fully by the Boltzmann and Saha distributions for excitations and ionizations. In reality, for conditions typical of stellar atmospheres, the colli-

sional rates do not dominate over the corresponding radiative rates, which is a pre-requisite for LTE to hold. Often it is therefore important to account for departures from LTE, which can be substantial in terms of derived abundances. The numerical techniques and codes to compute the statistical equilibrium in 1D have been available for decades, indeed even 3D non-LTE calculations are now feasible (e.g. Asplund et al. 2003). In spite of this, remarkably little work has been devoted to this important aspect of abundance analyses even in 1D. In fact, to date only a dozen or so elements have had their non-LTE line formation in solar-type atmospheres studied in some detail with contemporary atomic physics. Perhaps this can blamed on a notion within the astronomy community that the input physics is very uncertain. This is, however, only partly true, since the last decade has seen tremendous progress in this respect. Furthermore, it is possible to test the sensitivity of the outcome to the various rates, which can constrain the non-LTE effects. It is important to realize that LTE is more likely than not to be wrong with departures from LTE often being on the level of 0.1 dex for the Sun. Depending on the required accuracy in the derived abundances, LTE may or may not therefore be an acceptable approximation.

3. The Solar Photospheric Chemical Composition

The solar abundance analysis which is described below has been carried out using a 3D hydrodynamical model of the solar atmosphere (Asplund et al. 2000a). Both atomic and molecular lines of very different temperature and pressure sensitivities have been employed whenever possible in the hope that it should minimise systematic errors. A special effort has been made to utilise only the best available line data. In several incidences detailed non-LTE calculations have been carried out or the results thereof been culled from the literature. As a result, we are confident that the end-product is the most reliable element abundance analysis of the Sun carried out so far. Table 1 presents a compilation of the most reliable solar and meteoritic abundances in our opinion.

3.1. Lithium, Beryllium and Boron

Lithium is depleted in the solar convection zone by about a factor of 160 and as a consequence even the Li I resonance line at 670.8 nm is very weak (equivalent width $W_\lambda \simeq 0.18\,\mathrm{pm}{=}1.8\,\mathrm{m\AA}$); the subordinate line at 610.4 nm is hopelessly puny for the purpose of deriving a solar Li abundance. In addition, the 670.8 nm line is blended with CN and Fe I lines, which makes the determination of the solar Li abundance rather uncertain. Furthermore, Li I is a minority species, which is highly sensitive to both the temperature and the photo-ionizing UV radiation field (Kiselman 1997; Uitenbroek 1998). Our recommended solar Li abundance stems from the 1D LTE analysis by Müller et al. (1975). To this value we add the effects of atmospheric inhomogeneities and 3D non-LTE line formation (Asplund et al. 1999; Asplund et al. 2003; Barklem et al. 2003) and correct for a revised transition probability to arrive at $\log \epsilon_{\mathrm{Li}} = 1.05 \pm 0.10$.

Until recently Be was thought to be depleted in the solar photosphere by about a factor of two (Chiemlewski et al. 1975; Anders & Grevesse 1989). Balachandran & Bell (1998), however, revisited the issue by attempting to estimate any missing UV opacity and found a Be abundance from the Be II 313.1 nm reso-

Table 1. Element abundances in the present-day solar photosphere and in meteorites (C1 chondrites). Indirect solar estimates are marked with [..]

	Elem.	Photosphere	Meteorites		Elem.	Photosphere	Meteorites
1	H	12.00	8.25 ± 0.05	44	Ru	1.84 ± 0.07	1.77 ± 0.08
2	He	$[10.93 \pm 0.01]$	1.29	45	Rh	1.12 ± 0.12	1.07 ± 0.02
3	Li	1.05 ± 0.10	3.25 ± 0.06	46	Pd	1.69 ± 0.04	1.67 ± 0.02
4	Be	1.38 ± 0.09	1.38 ± 0.08	47	Ag	0.94 ± 0.24	1.20 ± 0.06
5	B	2.70 ± 0.20	2.75 ± 0.04	48	Cd	1.77 ± 0.11	1.71 ± 0.03
6	C	8.39 ± 0.05	7.40 ± 0.06	49	In	1.60 ± 0.20	0.80 ± 0.03
7	N	7.78 ± 0.06	6.25 ± 0.07	50	Sn	2.00 ± 0.30	2.08 ± 0.04
8	O	8.66 ± 0.05	8.39 ± 0.02	51	Sb	1.00 ± 0.30	1.03 ± 0.07
9	F	4.56 ± 0.30	4.43 ± 0.06	52	Te		2.19 ± 0.04
10	Ne	$[7.84 \pm 0.06]$	-1.06	53	I		1.51 ± 0.12
11	Na	6.17 ± 0.04	6.27 ± 0.03	54	Xe	$[2.27 \pm 0.02]$	-1.97
12	Mg	7.53 ± 0.09	7.53 ± 0.03	55	Cs		1.07 ± 0.03
13	Al	6.37 ± 0.06	6.43 ± 0.02	56	Ba	2.17 ± 0.07	2.16 ± 0.03
14	Si	7.51 ± 0.04	7.51 ± 0.02	57	La	1.13 ± 0.05	1.15 ± 0.06
15	P	5.36 ± 0.04	5.40 ± 0.04	58	Ce	1.58 ± 0.09	1.58 ± 0.02
16	S	7.14 ± 0.05	7.16 ± 0.04	59	Pr	0.71 ± 0.08	0.75 ± 0.03
17	Cl	5.50 ± 0.30	5.23 ± 0.06	60	Nd	1.45 ± 0.05	1.43 ± 0.03
18	Ar	$[6.18 \pm 0.08]$	-0.45	62	Sm	1.01 ± 0.06	0.92 ± 0.04
19	K	5.08 ± 0.07	5.06 ± 0.05	63	Eu	0.52 ± 0.06	0.49 ± 0.04
20	Ca	6.31 ± 0.04	6.29 ± 0.03	64	Gd	1.12 ± 0.04	1.03 ± 0.02
21	Sc	3.05 ± 0.08	3.04 ± 0.04	65	Tb	0.28 ± 0.30	0.28 ± 0.03
22	Ti	4.90 ± 0.06	4.89 ± 0.03	66	Dy	1.14 ± 0.08	1.10 ± 0.04
23	V	4.00 ± 0.02	3.97 ± 0.03	67	Ho	0.51 ± 0.10	0.46 ± 0.02
24	Cr	5.64 ± 0.10	5.63 ± 0.05	68	Er	0.93 ± 0.06	0.92 ± 0.03
25	Mn	5.39 ± 0.03	5.47 ± 0.03	69	Tm	0.00 ± 0.15	0.08 ± 0.06
26	Fe	7.45 ± 0.05	7.45 ± 0.03	70	Yb	1.08 ± 0.15	0.91 ± 0.03
27	Co	4.92 ± 0.08	4.86 ± 0.03	71	Lu	0.06 ± 0.10	0.06 ± 0.06
28	Ni	6.23 ± 0.04	6.19 ± 0.03	72	Hf	0.88 ± 0.08	0.74 ± 0.04
29	Cu	4.21 ± 0.04	4.23 ± 0.06	73	Ta		-0.17 ± 0.03
30	Zn	4.60 ± 0.03	4.61 ± 0.04	74	W	1.11 ± 0.15	0.62 ± 0.03
31	Ga	2.88 ± 0.10	3.07 ± 0.06	75	Re		0.23 ± 0.04
32	Ge	3.58 ± 0.05	3.59 ± 0.05	76	Os	1.45 ± 0.10	1.34 ± 0.03
33	As		2.29 ± 0.05	77	Ir	1.38 ± 0.05	1.32 ± 0.03
34	Se		3.33 ± 0.04	78	Pt		1.64 ± 0.03
35	Br		2.56 ± 0.09	79	Au	1.01 ± 0.15	0.80 ± 0.06
36	Kr	$[3.28 \pm 0.08]$	-2.27	80	Hg		1.13 ± 0.18
37	Rb	2.60 ± 0.15	2.33 ± 0.06	81	Tl	0.90 ± 0.20	0.78 ± 0.04
38	Sr	2.92 ± 0.05	2.88 ± 0.04	82	Pb	2.00 ± 0.06	2.02 ± 0.04
39	Y	2.21 ± 0.02	2.17 ± 0.04	83	Bi		0.65 ± 0.03
40	Zr	2.59 ± 0.04	2.57 ± 0.02	90	Th		0.06 ± 0.04
41	Nb	1.42 ± 0.06	1.39 ± 0.03	92	U	$<$-0.47	-0.52 ± 0.04
42	Mo	1.92 ± 0.05	1.96 ± 0.04				

nance doublet in agreement with the meteoritic value. There is a long-standing debate whether or not there is a need for additional continuous and/or line opacity in the UV spectral region over those already included in the model calculations in order to properly model the solar flux distribution. The novel feature with the analysis of Balachandran & Bell was their estimation of the amount of missing UV opacity by requiring that the OH A-X electronic lines around 313 nm should yield the same solar oxygen abundance as the OH vibration lines in the IR. In order to achieve this, they estimated that about 60% extra opacity was required, which they attributed largely to photo-ionization of Fe I (see also Bell et al. 2001). A follow-up study using a 3D solar model atmosphere instead of the MARCS (Gustafsson et al. 1975) and Holweger-Müller (1974) 1D models employed by Balachandran & Bell confirmed that Be is undepleted in the solar convection zone: $\log \epsilon_{\rm Be} = 1.38 \pm 0.09$ (Asplund 2004). It should be emphasized, however, that this result hinges completely on the correctness of the utilised method of estimating the missing opacity. In particular, departures from LTE for the OH A-X electronic lines could skew the results. No sufficiently detailed non-LTE calculation exists for these lines to our knowledge, which obviously is important in order to settle the issue. Likewise, improved determinations of the Fe I bound-free cross-sections would be very valuable.

The problem with possible missing UV opacity may also affect the determination of the solar B abundance, as the only available reliable indicator is the B I 249.67 nm resonance line. Cunha & Smith (1999) presented a re-analysis of the B I line, including a careful study of possible missing opacity sources such as photo-ionization of Mg I. Whilst the uncertainty in their result was relatively large, they found no evidence for a solar B depletion, which of course would be highly surprising if indeed Be is undepleted. We have estimated the 3D LTE effect (i.e. 3D LTE - 1D LTE) on the resonance line to be 0.04 dex in comparison with a solar MARCS or Kurucz model and -0.04 dex for the Holweger-Müller model. When also including departures from LTE as predicted by Kiselman & Carlsson (1996), we obtain $\log \epsilon_{\rm B} = 2.70 \pm 0.20$. The large uncertainty is dominated by the problem in analysing this very crowded spectral region.

3.2. Carbon

The solar carbon abundance can be determined from a wide range of indicators, both atomic and molecular transitions. We have recently performed a detailed study of the best abundance diagnostics in our opinion: the forbidden [C I] 872.7 nm line, high excitation C I lines, CH vibration-rotation IR lines, CH A-X electronic lines, C_2 Swan electronic lines and CO vibration lines (Allende Prieto et al. 2002; Asplund et al. 2004b; Scott et al., in preparation). The line formation was computed based on a 3D hydrodynamical model of the solar atmosphere (Asplund et al. 2000a) and departures from LTE were accounted for in the case of the C I lines. In sharp contrast with analyses using 1D model atmospheres, very gratifying agreement is found between all abundance indicators when employing the 3D model, as clear from Table 2. Given the extreme temperature sensitivity of molecule formation, it is crucial to include the effects of atmospheric inhomogeneities for the molecular lines in order not to estimate too high abundances, which is the case with 1D models. Our new solar C abundance of $\log \epsilon_{\rm C} = 8.39 \pm 0.05$ is 0.17 dex lower than the recommended value in

Table 2. The derived solar C, N and O abundances as implied by a variety of different atomic and molecular indicators using a 3D hydrodynamical model of the solar atmosphere (Asplund et al. 2004a,b; Asplund et al., in preparation; Scott et al., in preparation). In addition, the corresponding results for two 1D model atmospheres, a theoretical MARCS (Asplund et al. 1997) and the semi-empirical model of Holweger-Müller (1974), are given for comparison purposes. Note the excellent agreement between atomic and molecular diagnostics with the 3D model and the large spread when using 1D model atmospheres. The quoted uncertainty is only the line-to-line scatter; no error is given for [C I] as the result is based only on the 872.7 nm line. The O abundance used for the CO calculations was 8.66 in the case of 3D and 8.85 for the two 1D models

lines	$\log\epsilon_{\rm C,N,O}$		
	3D	HM	MARCS
[C I]	8.39	8.45	8.40
C I	8.36 ± 0.03	8.39 ± 0.03	8.35 ± 0.03
CH $\Delta v = 1$	8.38 ± 0.04	8.53 ± 0.04	8.42 ± 0.04
C_2 Swan	8.44 ± 0.03	8.53 ± 0.03	8.46 ± 0.03
CH A-X	8.45 ± 0.04	8.59 ± 0.04	8.44 ± 0.04
CO $\Delta v = 1$	8.41 ± 0.02	8.62 ± 0.02	8.57 ± 0.02
CO $\Delta v = 2$	8.38 ± 0.02	8.70 ± 0.03	8.59 ± 0.03
N I	7.85 ± 0.08	7.97 ± 0.08	7.94 ± 0.08
NH $\Delta v = 1$	7.73 ± 0.05	7.95 ± 0.05	7.82 ± 0.05
[O I]	8.68 ± 0.01	8.76 ± 0.02	8.72 ± 0.01
O I	8.64 ± 0.02	8.64 ± 0.08	8.72 ± 0.03
OH $\Delta v = 0$	8.65 ± 0.02	8.82 ± 0.01	8.83 ± 0.03
OH $\Delta v = 1$	8.61 ± 0.03	8.87 ± 0.03	8.74 ± 0.03

the widely used compilation of Anders & Grevesse (1989). The excellent agreement between transitions of very different formation depths and temperature and pressure sensitivities is a very strong argument in favour of this low abundance as well as for the realism of the 3D model. In particular we note with satisfaction that consistent results are now finally provided also by the CO lines, which have previously caused a great deal of trouble when analysed within the framework of 1D model atmospheres (Grevesse et al. 1995; Ayres 2002 and references therein).

A 3D analysis of weak $^{12}C^{16}O$ and $^{13}C^{16}O$ lines yields a photospheric $^{12}C/^{13}C$ ratio of 95 ± 5 (Scott et al., in preparation), which is in excellent agreement with telluric measurements (Rosman & Taylor 1998).

3.3. Nitrogen

We have recently re-determined the solar N abundance on the basis of the same 3D hydrodynamical model atmosphere as previously used for the corresponding C and O analyses (Asplund et al, in preparation). In the case of N there are

fewer abundance indicators compared with its two neighboring elements. We have utilised N I and NH vibration-rotation lines while relegating the CN red band to a supporting role. The N I list consists of 21 weak ($W_\lambda = 0.1 - 1\,\mathrm{pm}$), high-excitation ($\chi_{\mathrm{exc}} = 10.3 - 12.4\,\mathrm{eV}$) lines, which implies a 3D LTE abundance of $\log \epsilon_{\mathrm{N}} = 7.88 \pm 0.08$. No 3D non-LTE study for N is as yet available but the application of the computed 1D non-LTE abundance corrections by Rentzsch-Holm (1996) lowers this abundance to $\log \epsilon_{\mathrm{N}} = 7.85 \pm 0.08$. It should be noted, however, that Rentzsch-Holm (1996) employs efficient inelastic H collisions, which help thermalise the level populations. Given that the available laboratory and quantum mechanical calculations tend to suggest that the classical recipe used by her significantly over-estimates the H collision cross-sections (e.g. Belyaev et al. 1999; Barklem et al. 2003), the N I based abundance presented here may require a small downward revision.

We have also used a sample of 22 weak NH vibration-rotation lines in the IR (located around 3μm), which have previously been advocated as primary abundance indicators (Grevesse et al. 1990). As with all molecular lines, the NH lines are very temperature sensitive and as consequence there is a large difference between the results of 1D and 3D analyses. The NH lines indicate an abundance of $\log \epsilon_{\mathrm{N}} = 7.73 \pm 0.05$ with our 3D solar model, which is significantly lower than with the standard Holweger-Müller 1D model.

3.4. Oxygen

Allende Prieto et al. (2001) argued for a significantly lower solar O abundance than the then widely accepted value, largely due to the presence of a previously unaccounted for blend in the forbidden [O I] 630.0 nm line. We have subsequently performed a much more detailed study, which also included high-excitation permitted O I lines and molecular transitions of OH, both vibration-rotation and pure rotation lines (Asplund et al. 2004a). As the O I lines are known to be susceptible to non-LTE effects, full 3D non-LTE line formation calculations were performed for these lines. It has long been clear that the OH lines imply higher abundance by about 0.2 dex than the O I lines when including departures from LTE, regardless of which 1D model atmosphere has been used. Finally this problem has been resolved with the application of 3D hydrodynamical models. The agreement between the various atomic and molecular lines is excellent, in spite of their very different atmospheric sensitivities. The almost perfect match between predicted and observed line profiles and center-to-limb variations provides further evidence that the 3D model is highly realistic. Furthermore, Melendez (2004) finds a similarly low O abundance from the extremely weak first overtone OH vibration lines, which have previously not been used.

A 3D analysis of isotopic CO lines yields a photospheric $^{16}\mathrm{O}/^{18}\mathrm{O}$ ratio of 530 ± 40 (Scott et al., in preparation), which is in good agreement with the telluric data (Rosman & Taylor 1998).

3.5. Neon and Argon

The photospheric abundances of Ne and Ar can not be determined directly due to the lack of suitable spectral lines. Their recommended values in Table 1 have been estimated from measured abundance ratios in the solar corona and solar energetic particles in conjunction with the photospheric abundance for

the reference element, which in this case is O. The Ne and Ar abundances are therefore directly affected by the revised solar O abundance. This explains most of the difference compared with for example Anders & Grevesse (1989) with a secondary effect coming from refined coronal abundance ratio determinations (Reames 1999).

3.6. Sodium to Calcium

In connection with the present conference, we have performed a preliminary 3D LTE abundance analysis for the remaining elements up to calcium. We have been heavily influenced by the study of Lambert & Luck (1978) who performed a similar analysis using the Holweger-Müller (1974) semi-empirical 1D model atmosphere. In particular our choice of lines has been largely moulded by their recommendations, with the added constraint that we have so far restricted the comparison to only weak lines. Line profile fitting has been used in all cases to estimate the abundance instead of equivalent widths. We have ransacked the recent literature for the most up-to-date transition probabilities. As appropriate, we take into account departures from LTE, although computed for 1D models since full 3D non-LTE calculations for these elements are well beyond the scope of the present study. While this is inconsistent in principle it is expected to give at least a good first estimate of the 3D non-LTE effects (Asplund et al. 2004a). Space permits only a very brief summary here with the full details being presented elsewhere (Asplund et al., in preparation). The preliminary results are listed in Table 1. The new 3D-based abundance are in all cases slightly lower than those recommended by Anders & Grevesse (1989) and Grevesse & Sauval (1998), the difference being typically $0.05 - 0.10$ dex. The impact of the 3D model atmosphere is thus smaller here than for C, N and O, mainly since these abundances are based on atomic transitions rather than very temperature sensitive molecular lines.

The Na abundance is based on six weak Na I lines. The computed non-LTE abundance corrections are small (< 0.05 dex) but slightly lower the mean abundance to $\log \epsilon_{\rm Na} = 6.17 \pm 0.04$, which is 0.1 dex lower than the meteoritic value. As the gf-values should be reliable, an explanation for this minor discrepancy has not yet been identified. The transition probabilities for Mg I are notoriously uncertain, forcing the Mg abundance to be estimated from four Mg II lines: $\log \epsilon_{\rm Mg} = 7.53 \pm 0.09$. Non-LTE effects should be negligible for Mg II. The Mg I value is very similar but with unacceptably large uncertainties. Many Al I lines are detected in the solar spectrum but the majority give quite discrepant results, mainly due to cancellation and configuration interaction effects in the calculations of the gf-values. We consider only four Al I lines to be of sufficiently high quality for this purpose, which suggests $\log \epsilon_{\rm Al} = 6.37 \pm 0.06$. Based on the published departure coefficients by Baumüller & Gehren (1996), possible non-LTE effects should be minor for these relatively high-excitation lines. The Si abundance is that of Asplund (2000).

Our recommended P abundance stems from an analysis of five P I lines in the near-IR with equivalent widths $W_\lambda < 2.5$ pm. With the gf-values of Berzinsh et al. (1997) we find $\log \epsilon_{\rm P} = 5.36 \pm 0.04$. From the line list used by Lambert & Luck (1978), we removed several S I lines with profiles that indicate blends. The pruned list of ten lines indicate $\log \epsilon_{\rm S} = 7.14 \pm 0.05$. The new S abundance

is now in excellent agreement with the meteoritic value. Chlorine, like fluorine, has not been possible to analyse with our 3D model atmosphere of quiet Sun as the relevant HCl lines are only present in sunspot spectra. The highly uncertain Cl abundance dates back to Hall & Noyes (1972). As we have restricted the analysis to weak and intermediate strong lines, we have not yet used the very strong K I 769.8 nm resonance line and instead base our K abundance on five weak K I transitions at 404.4, 580.1, 1176.9, 1243.2 and 1252.2 nm. Together with the non-LTE abundance corrections of Ivanova & Shimanskii (2000), these lines imply $\log \epsilon_{\rm K} = 5.08 \pm 0.07$. Finally, for Ca a nice selection of both permitted and forbidden Ca I transitions as well as Ca II lines are available in the solar spectrum. The agreement between the two ionization stages is excellent, and we simply take the average of the two: $\log \epsilon_{\rm Ca} = 6.31 \pm 0.04$.

3.7. Other Elements

Of the remaining elements, only Fe has been the topic of a 3D abundance analysis (Asplund et al. 2000b), whose value we adopt here: $\log \epsilon_{\rm Fe} = 7.45 \pm 0.05$. Almost identical abundances are suggested by Fe I and Fe II lines. We note that this value has not been corrected for departures from LTE. Shchukina & Trujillo Bueno (2001) found that the Fe I based abundance should be adjusted upwards by about 0.05 dex based on 1.5D (i.e. only including vertical radiative transfer and therefore treating each atmospheric column as a separate 1D model atmosphere) non-LTE calculations using one snapshot from the 3D solar model used here. Their calculations did not include any inelastic H collisions, which would tend to decrease the non-LTE effects towards restoring the LTE results. The jury is still out whether or not these collisions are efficient. Korn et al. (2003) present convincing arguments that they are in the case of Fe, and we therefore tentatively recommend the 3D LTE value. Clearly, detailed quantum mechanical calculations for Fe+H collisions are very important but unfortunately the task is extremely challenging.

While no 3D studies have been carried out for the remaining elements, the recommended values in Table 1 nevertheless differ in several incidences compared with previous compilations. This is largely the result of the very important work done by a small group of dedicated atomic physicists in measuring and calculating improved transition probabilities. Much recent attention has been devoted to the heavy elements formed by neutron capture, like La (Lawler et al. 2001a), Nd (Den Hartog et al. 2003), Eu (Lawler et al. 2001c), Tb (Lawler et al. 2001b), Ho (Lawler et al. 2004), Pt (Den Hartog et al. 2004) and Pb (Biémont et al. 2000). Some beautiful examples of this are shown in Sneden et al. (these proceedings). Some other elements whose abundances have been revised due to improved atomic data and/or line selection in recent years are Ti, Ni (Reddy et al. 2003), Ge (Biémont et al. 1999) and Sr (Barklem & O'Mara 2000).

Finally, we note that we have not here attempted to homogenise the rather diverse collection of photospheric abundances presented in Table 1. They have not all been derived using the same model atmosphere, departures from LTE have only occasionally been accounted for and the methods for estimating the attached uncertainties differ between authors. This should be borne in mind by the prospective users of this data.

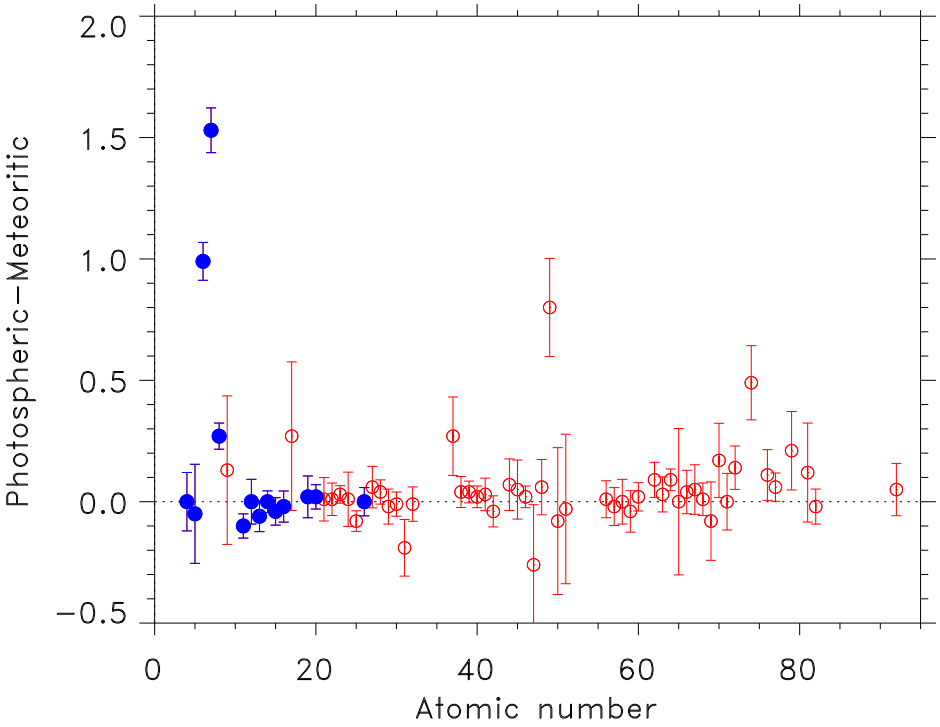

Figure 1. Comparison of photospheric and meteoritic abundances (as measured in C1 chondrites). The elements which have been analysed using a 3D hydrodynamical solar model atmosphere are shown as filled circles while the 1D-based results with open circles. H, Li and the noble gases all fall outside the figure due to significant depletion either in the Sun or in the meteorites, which also affects C, N and O

4. Comparison with the Meteoritic Evidence

In Table 1 we also present a compilation of meteoritic abundances as measured in C1 chondrites. The data is largely taken from Lodders (2003) but placed on a slightly different absolute abundance scale. It is important to realize that since H, like other volatile elements, is highly depleted in meteorites, another reference element must be found. The honour is normally given to Si. As a consequence, in order to anchor the meteoritic and photospheric absolute abundance scales to each other a knowledge of the photospheric Si abundance is required. Since our recommended value is 0.03 dex lower than that advocated by Lodders (2003), we correspondingly adjust all meteoritic abundances by this amount.

Fig. 1 shows the difference between the photospheric and meteoritic abundances. In general the agreement is very good. Some notable differences can be easily explained by depletion in the Sun (Li) or in the meteorites (H, C, N, O and the noble gases). In addition there are a small number of elements which show discordant results: Ga, Rb, Ag, In and W, with Cl and Au only barely agreeing within the large uncertainties. In the case of In and W one may suspect

unidentified blends being the cause of the discrepancies given that the photospheric abundances are significantly higher than the meteoritic values. For the other problematic elements erroneous gf-values or departures from LTE may be to blame. As mentioned above, the new Na abundance does not overlap with the meteoritic value. Although the difference is only 0.1 dex, this deserves further investigation. The mean difference for the non-depleted elements is 0.01 ± 0.06 dex, when ignoring the above-mentioned seven elements.

5. Trouble in Paradise?

The new solar abundances described here have some important ramifications.

The first one is evident from the abundances by mass of H, He and metals, X, Y and Z, which now become $X = 0.7392$, $Y = 0.2486$ and $Z = 0.0122$ with $Z/X = 0.0165$, i.e. much lower metallicity and Z/X than previously recommended (e.g. $Z/X = 0.0275$ from Anders & Grevesse 1989). These are the present-day photospheric values with the He abundance taken from Basu & Antia (2004).

The low solar C and O abundances are now in much better agreement with those measured in the local interstellar medium (e.g. André et al. 2003) as well as for nearby B stars (e.g. Sofia & Meyer 2001). Previously the high solar abundances apparently already in place 4.5 Gyr ago were inconsistent with the low values found in the solar neighborhood today in the framework of Galactic chemical evolution. Somewhat surprisingly, the problem appears to have been in the solar determination rather than in the analyses of nebulae and hot stars.

While the new abundances may have solved some long-standing problems, it also introduces at least one new, namely for helioseismology. Over the years, standard solar interior models which account for element settling have yielded an impressive agreement with the observed sound speed in the Sun as measured by the solar oscillations. Since C, N, O and Ne are important opacity contributors, the revised solar abundances for these elements significantly alter the interior structure. Indeed the predicted sound speed in these new solar models are in much worse agreement with helioseismology (Bahcall et al. 2004; Basu & Antia 2004). According to these authors, the only possible culprits are the new photospheric abundances or the opacities, having discarded the possibility of underestimated element settling in the solar models. The necessary opacity increase near the bottom of the convection zone is significant, at least 10%. Some of this may in fact already have been found (Seaton & Badnell 2004), but more than half still remains. Whether the fault lies entirely with the opacity calculations or whether our new abundances are in fact underestimated is an open question, which urgently needs to be resolved. Experience constantly reminds us that one should never claim anything as impossible, but we consider it unlikely that our derived abundances are as far from the real values as suggested by these helioseismology studies. It would be a remarkable conspiracy of factors if this was the case, considering that the atomic and molecular-based abundances now finally agree, the lack of any significant trends in derived abundances with for example line strength or excitation potential and the almost perfect match between observed and predicted line profiles, including their asymmetries. The employed lines in our work probe very different parts of the solar atmospheric

with greatly different sensitivities to the atmospheric conditions, which implies that a great deal of fine-tuning would be necessary to simultaneously bring the C, N and O abundances up by some 0.2 dex, if at all possible. As mentioned above, the new abundances also removes the special nature the Sun otherwise would have in comparison with its neighborhood.

6. Concluding Remarks

Although progress has been made in refining our knowledge of the solar chemical composition, much work still remains. An obvious way forward is to extend the 3D analysis presented here to the remaining elements in the periodic table. Furthermore, the lack of detailed non-LTE line formation calculations is a major cause of concern, not only for the solar abundance determinations but also for much of the stellar work. Equally important, however, is continued investment in improving the necessary atomic and molecular data. Although the impact may not be as profound as the recent surprisingly large revisions of the solar metal content, efforts along these lines would nevertheless be worthwhile.

Acknowledgments. It is a great pleasure to pay tribute to David Lambert for all of his many important contributions to stellar spectroscopy and his unique ability to bridge the gap to the nuclear and atomic physics communities. Among his many achievements we would like to here high-light his several seminal papers on the solar chemical composition, which to a great extent have shown the way for very accurate abundance determinations. We would also like to thank our various collaborators related to this work, including Carlos Allende Prieto, Paul Barklem, Ronny Blomme, Mats Carlsson, Dan Kiselman, David Lambert, Åke Nordlund, Pat Scott, Bob Stein and Regner Trampedach. MA and NG gratefully acknowledge financial support from the SOC/LOC.

References

Allende Prieto, C., García López, R.J., Lambert, D.L., et al. 2000, ApJ, 528, 885
Allende Prieto, C., Lambert, D.L., & Asplund, M. 2001, ApJ, 556, L63
Allende Prieto, C., Lambert, D.L., & Asplund, M. 2002, ApJ, 573, L137
Anders, E., & Grevesse, N. 1989, Geochim. Cosmochim. Acta, 53, 197
André, M.K., Oliveira, C.M., Howk, J.C., et al. 2003, ApJ, 591, 936
Asplund, M. 2000, A&A, 359, 755
Asplund, M. 2004, A&A, 417, 769
Asplund, M., & García Pérez, A.E. 2001, A&A, 372, 601
Asplund, M., Carlsson, M., & Botnen, A.V. 2003, A&A, 399, L31
Asplund, M., Grevesse, N., Sauval, A.J., et al. 2004a, A&A, 417, 751
Asplund, M., Grevesse, N., Sauval, A.J., et al. 2004b, A&A, submitted
Asplund, M., Gustafsson, B., Kiselman, D., & Eriksson, K. 1997, A&A, 318, 521
Asplund, M., Nordlund, Å., Trampedach, R., & Stein, R.F. 1999, A&A, 346, L17
Asplund, M., Nordlund, Å., Trampedach, R., et al. 2000a, A&A, 359, 729
Asplund, M., Nordlund, Å., Trampedach, R., & Stein R.F. 2000b, A&A, 359, 743
Atroshchenko, I.N., & Gadun, A.S. 1994, A&A, 291, 635
Ayres, T.R. 2002, ApJ, 575, 1104
Bahcall, J.N., Basu, S., Pinsonneault, M., & Serenelli, A.M., 2004, ApJ, in press
Balachandran, S., & Bell, R.A. 1998, Nature, 392, 23
Barklem, P.S., Belyaev, A., & Asplund, M. 2003, A&A, 409, L1

Barklem, P.S., & O'Mara, B.J. 2000, MNRAS, 311, 535
Basu, S., & Antia, H.M. 2004, ApJ, 606, L85
Baumüller, D., & Gehren, T. 1996, A&A, 307, 961
Bell, R.A., Balachandran, S., & Bautista, M.A. 2001, ApJ, 546, L65
Belyaev, A.K., Grosser, J., Hahne, J., & Menzel, T. 1999, Phys.Rev.A, 60, 2151
Berzinsh, U., Svanberg, S., & Biémont, E. 1997, A&A, 326, 412
Biémont, E., Garnir, H.P., Palmeri, P., et al. 2000, MNRAS, 312, 116
Biémont, E., Lynga, C., Li, Z.S., et al. 1999, MNRAS, 303, 721
Böhm-Vitense, E. 1958, Z. Astroph., 46, 108
Canuto, V.M., & Mazzitelli, I. 1991, ApJ, 370, 295
Chiemlewski, Y., Müller, E.A., & Brault, J.M. 1975, A&A, 42, 37
Cunha, K., & Smith, V.V. 1999, ApJ, 512, 1006
Cunto, W., Mendoza, C., Ochsenbein, F., & Zeippen, C.J. 1993, A&A, 275, L5
Den Hartog, E.A., Herd, M.T., Lawler, et al. 2004, ApJ, in press
Den Hartog, E.A., Lawler, J.E., Sneden, C., & Cowan, J.J. 2003, ApJS, 148, 543
Dravins, D., & Nordlund, Å. 1990, A&A, 228, 184
Grevesse, N., & Sauval, A.J. 1998, Space Sci. Rev., 85, 161
Grevesse N., Noels A., & Sauval A.J. 1995, in ASP Conference Series, Vol. 81, Laboratory and Astronomical High Resolution Spectra, eds. A.J. Sauval, R. Blomme, & N. Grevesse, San Francisco, 74
Grevesse, N., Lambert, D.L., Sauval, A.J., et al. 1990, A&A, 232, 225
Gustafsson, B., Bell, R.A., Eriksson, K., & Nordlund, Å. 1975, A&A, 42, 407
Hall, D.N.B., & Noyes, R.W. 1972, ApJ, 175, L95
Hauschildt, P., Allard, F., & Baron, E. 1999, ApJ, 512, 377
Holweger, H., & Müller, E.A. 1974, Sol. Phys., 39, 19
Ivanova, D.V., & Shimanskii, V.V. 2000, Ast. Reports, 44, 376
Kiselman, D. 1997, ApJ, 489, L107
Kiselman, D., & Carlsson, M. 1996, A&A, 311, 680
Korn, A., Shi, J., & Gehren, T. 2003, A&A, 407, 691
Kurucz, R.L. 1979, ApJS, 40, 1
Kurucz, R.L. 1993, CD-ROM, private communication
Lambert, D.L., & Luck, R.E. 1978, MNRAS, 183, 79
Lawler, J.E., Sneden, C., & Cowan, J.J. 2004, ApJ, 604, 850
Lawler, J.E., Bonvallet, G., & Sneden, C. 2001a, ApJ, 556, 452
Lawler, J.E., Wickliffe, M.E., Cowley, C.R., & Sneden, C. 2001b, ApJS, 137, 341
Lawler, J.E., Wickliffe, M.E., den Hartog, E. A., & Sneden, C. 2001c, ApJ, 563, 1075
Lodders, K. 2003, ApJ, 591, 1220
Melendez, J. 2004, ApJ, in press [astro-ph/0407366]
Mihalas, D., Däppen, W., & Hummer, D.G. 1988, ApJ, 331, 815
Müller, E.A., Peytremann, E., & de la Reza, R. 1975, Sol. Phys., 41, 53
Nordlund, Å. 1982, A&A, 107, 1
Nordlund, Å., & Dravins, D. 1990, A&A, 228, 155
Reames, D.V. 1999, Space Sci. Rev., 90, 413
Reddy, B.E., Tomkin, J., Lambert, D.L., & Allende Prieto, C. 2003, MNRAS, 340, 304
Rentzsch-Holm, I. 1996, A&A, 305, 275
Rosman, K.J.R., & Taylor, P.D.P. 1998, Pure & Appl. Chem., 70, 217
Seaton, M.J., & Badnell, N.R. 2004, MNRAS, in press [astro-ph/0404437]
Shchukina, N., & Trujillo Bueno, J. 2001, ApJ, 550, 970
Sofia, U.J., & Meyer, D.M. 2001, ApJ, 554, L221
Steffen, M., & Holweger, H. 2002, A&A, 387, 258
Steffen, M, Ludwig, H.-G., & Freytag, B. 1995, A&A, 300, 473
Stein, R.F., & Nordlund, Å. 1998, ApJ, 499, 914
Uitenbroek, H. 1998, ApJ, 498, 427
Vernazza, J.E., Avrett, E.H., & Loeser, R. 1976, ApJS, 30, 1
Vögler, A., Bruls, J.H.M.J., & Schüssler, M. 2004, A&A, 421, 741